IOP Publishing New J. Phys. 18 (2016) 093024 doi:10.1088/1367-2630/18/9/093024

New Journal of Physics
The open access journal at the forefront of physics

Deutsche Physikalische Gesellschaft DPG
IOP Institute of Physics

Published in partnership with: Deutsche Physikalische Gesellschaft and the Institute of Physics

PAPER

OPEN ACCESS

RECEIVED
26 July 2016

REVISED
23 August 2016

ACCEPTED FOR PUBLICATION
30 August 2016

PUBLISHED
14 September 2016

A hybrid superconducting quantum dot acting as an efficient charge and spin Seebeck diode

Sun-Yong Hwang, David Sánchez and Rosa López

Institut de Física Interdisciplinària i Sistemes Complexos IFISC (UIB-CSIC), E-07122 Palma de Mallorca, Spain

E-mail: david.sanchez@uib.es

Keywords: quantum thermoelectrics, thermoelectric diode, spin Seebeck diode, hybrid quantum dot, nonlinear quantum transport

Abstract

We propose a highly efficient thermoelectric diode device built from the coupling of a quantum dot with a normal or ferromagnetic electrode and a superconducting reservoir. The current shows a strongly nonlinear behavior in the forward direction (positive thermal gradients) while it almost vanishes in the backward direction (negative thermal gradients). Our discussion is supported by a gauge-invariant current-conserving transport theory accounting for electron–electron interactions inside the dot. We find that the diode behavior is greatly tuned with external gate potentials, Zeeman splittings or lead magnetizations. Our results are thus relevant for the search of novel thermoelectric devices with enhanced functionalities.

1. Introduction

Diodes are building blocks in modern electronics industry due to its ability to show unidirectional current flow. Thus, in semiconductor p–n junctions the current I becomes a non-odd function of the applied voltage V, $I(V) \neq -I(-V)$, leading to substantial rectification. Recently, the interest has shifted to finding diode effects in devices in the presence of a thermal gradient θ [1], $I(\theta) \neq -I(-\theta)$. This is a thermoelectric phenomenon and thereby the name of Seebeck diodes. Furthermore, the spin current can be also rectified as predicted in the spin Seebeck diodes [2–6]. Here, the spin current is generated via the experimentally demonstrated spin Seebeck effect [7–9].

In quantum coherent conductors coupled to normal metallic leads, the thermoelectric current becomes strongly nonlinear when the local density of states is energy dependent and more than one resonance is involved in the transmission function [10, 11]. Otherwise, the weakly nonlinear terms in a current–temperature expansion are small compared to the linear response coefficients [12, 13]. These nonlinearities precisely describe, to leading order, rectification and diode effects [14]. We have recently shown that a quantum dot sandwiched between ferromagnetic and superconducting terminals exhibits large thermoelectric power and figure of merit [15]. The effect arises because a spin-split dot level allows for tunneling from the hot metallic lead to the available quasiparticle states in the cold superconducting side [16–19]. Nevertheless, our analysis was valid in the linear regime of transport only. In this paper, we consider the nonlinear case. Surprisingly, we find a highly efficient diode effect that works equally well for both the charge and the spin transport flow. The basic operating principle of our device relies on a strong energy dependence of the transmission function which naturally arises in the quasiparticle spectrum of normal-superconducting junction.

A careful calculation of the current–voltage characteristics beyond linear response requires knowledge of the nonequilibrium screening potential inside the mesoscopic structure [20]. When the nanosystem is subjected to the application of large thermal gradients, one needs to determine the variation of the internal electrostatic field to temperature shifts [12, 21, 22]. For large quantum dots or for dots strongly coupled to the leads (weak Coulomb blockade regime [23]), it suffices to treat electron–electron interactions at the mean-field level. We consider a single-level dot with fluctuating potential U due to injected charges from the attached leads, see figure 1. A recent work reports the observation of weak diode effects in a superconductor coupled to a two-dimensional electron gas [24]. We here propose that a hybrid quantum dot working as an energy filter between

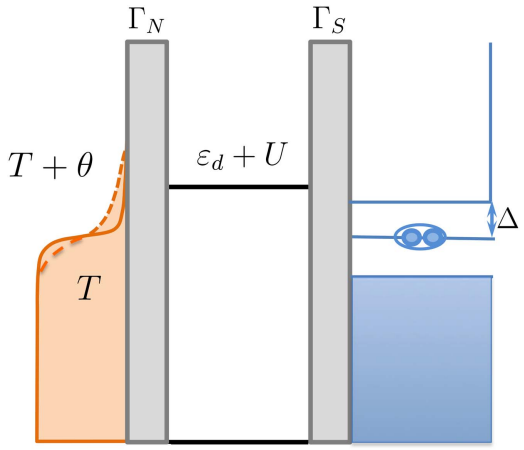

Figure 1. Sketch of our Seebeck diode. Left normal (N) or ferromagnetic (F) lead can be heated or cooled, which respectively generates thermal broadening (dashed orange line) or sharpening (full orange line) of the Fermi function. The right superconductor (S) maintains the thermal equilibrium. As a consequence, at low background temperature T the states below the gap are filled (blue color). The energy level $\varepsilon_{\rm d}$ of the quantum dot sandwiched between tunnel barriers (gray color) of transparencies $\Gamma_{\rm N}$ and $\Gamma_{\rm S}$ can be renormalized by interaction U and tunable by a back gate potential away from the Fermi energy (blue line). The potential U shifts upward as the forward thermal bias ($\theta > 0$) is applied creating a synergetic effect on the strongly nonlinear current with the thermally excited quaisiparticles from the left lead. On the other hand, cooling with a backward thermal bias ($\theta < 0$) lowers the current as the number of available states sharply decreases.

the normal reservoir and the superconducting terminal [25, 26] leads to much stronger diode features with rectification efficiencies close to unity.

2. Formalism

Our Seebeck diode consists of a ferromagnetic (F) reservoir characterized by a spin-polarization p ($|p| \leqslant 1$), a single-level quantum dot (D), and the superconductor (S), as depicted in figure 1. The normal metal case (N) has equal spin up and down densities, we therefore put $p = 0$ in the left lead. We write the model Hamiltonian [27]

$$\mathcal{H} = \mathcal{H}_{\rm L} + \mathcal{H}_{\rm S} + \mathcal{H}_{\rm D} + \mathcal{H}_{\rm T}, \tag{1}$$

where

$$\mathcal{H}_{\rm L\ =\ N,F} = \sum_{k\sigma} \varepsilon_{{\rm L}k\sigma} c^{\dagger}_{{\rm L}k\sigma} c_{{\rm L}k\sigma} \tag{2}$$

describes the left N or F lead with charge carriers of momentum k, spin $\sigma = \uparrow, \downarrow$, and energy $\varepsilon_{{\rm L}k\sigma}$, and

$$\mathcal{H}_{\rm S} = \sum_{k\sigma} \varepsilon_{{\rm S}k\sigma} c^{\dagger}_{{\rm S}k\sigma} c_{{\rm S}k\sigma} + \sum_{k} [\Delta c^{\dagger}_{{\rm S}k\uparrow} c^{\dagger}_{{\rm S},-k\downarrow} + {\rm h.c.}] \tag{3}$$

is the superconductor Hamiltonian with the energy gap Δ. We consider an equilibrium superconductor where the phase of Δ can be neglected by a gauge transformation, hence void of AC Josephson effect arising from the phase evolution. Importantly, in the dot Hamiltonian of equation (1)

$$\mathcal{H}_{\rm D} = \sum_{\sigma} (\varepsilon_{{\rm d}\sigma} + U_{\sigma}) d^{\dagger}_{\sigma} d_{\sigma}, \tag{4}$$

the spin-dependent energy level $\varepsilon_{{\rm d}\sigma} = \varepsilon_{\rm d} + \sigma\Delta_Z$ is renormalized by the internal potential U_{σ} that accounts for the Coulomb interaction. The Zeeman splitting Δ_Z is finite when the magnetic field is on. The screening potential $U = \sum_{\sigma} U_{\sigma}$ is determined by solving the Poisson's equation which for homogeneous potentials reads $\delta q = q - q_{\rm eq} = C(U - V_{\rm g})$ where C and $V_{\rm g}$ are the capacitance of the dot and the gate potential applied to it, respectively. We consider the charge neutral limit ($C = 0$), an experimentally relevant situation for strongly interacting dots. The solution can be expressed by the lesser Green's function [28], i.e., $q = -{\rm i}\int {\rm d}\varepsilon G^{<}(\varepsilon)$, where $G^{<}(t, t') = {\rm i}\langle {\rm d}^{\dagger}(t'){\rm d}(t)\rangle$. We also consider the spin-generalized case [27] and solve the Poisson's equation in a spin-dependent manner [29] incorporating the ferromagnet polarization and the magnetic field applied to the quantum dot. In this case, the spin-dependent charge density reads $q_{\sigma} = -{\rm i}\int {\rm d}\varepsilon G^{<}_{\sigma}(\varepsilon)$ where $G^{<}_{\sigma}(\varepsilon)$ is explicitly written in appendix. In order to take into account full nonlinearity of the temperature gradient θ (figure 1), we numerically solve two nonlinear equations

$$\delta q_{\uparrow}(\theta, U_{\uparrow}, U_{\downarrow}) = \delta q_{\downarrow}(\theta, U_{\uparrow}, U_{\downarrow}) = 0. \tag{5}$$

Here, the screening potential fluctuates in order to keep the dot charge constant. This gives the solution of the form $U_\sigma = U_\sigma(\theta)$ for each spin $\sigma = \uparrow, \downarrow$ valid to all orders in a temperature expansion of the potential. We find that interactions favor the diode effect. This will be discussed more in detail below. Finally, the tunneling Hamiltonian in equation (1) reads

$$\mathcal{H}_{\rm T} = \sum_{k\sigma} t_{{\rm L}\sigma} c^{\dagger}_{{\rm L}k\sigma} d_\sigma + \sum_{k\sigma} t_{{\rm S}\sigma} c^{\dagger}_{{\rm S}k\sigma} d_\sigma + {\rm h.c.}, \tag{6}$$

where $t_{\alpha\sigma}$ is the hopping amplitude between the quantum dot and each lead $\alpha = {\rm L}, {\rm S}$.

The spin-resolved current $I_\sigma = -({\rm i}e/\hbar)\langle[\mathcal{H}, N_{{\rm L}\sigma}]\rangle$ can be evaluated from the time evolution of electron number $N_{{\rm L}\sigma} = \sum_k c^{\dagger}_{{\rm L}k\sigma} c_{{\rm L}k\sigma}$ in the left lead by employing the nonequilibrium Keldysh Green's function technique [30, 31]. In the isoelectric case with no voltage bias $V = 0$, the subgap Andreev current is completely blocked since $I^\sigma_{\rm A} = (e/h)\int {\rm d}\varepsilon T^\sigma_{\rm A}(\varepsilon)[f_{\rm L}(\varepsilon - eV) - f_{\rm L}(\varepsilon + eV)]$ is identically zero to all orders in θ [32]. This insensitivity of $I^\sigma_{\rm A}$ to thermal gradients only is a manifestation of the particle-hole symmetry inherent in the subgap transport. Consequently, the total current emerges only from the quasiparticle contribution; hence we can write the spin-resolved current

$$I_\sigma = \frac{e}{h}\int {\rm d}\varepsilon \;\; T^\sigma_{\rm Q}(\varepsilon)[f_{\rm L}(\varepsilon) - f_{\rm S}(\varepsilon)], \tag{7}$$

where $f_{\alpha={\rm L,S}}(\varepsilon) = \{1 + \exp[(\varepsilon - E_{\rm F})/k_{\rm B}T_\alpha]\}^{-1}$ is the Fermi–Dirac distribution function with local temperature for each lead $T_\alpha = T + \theta_\alpha$ (T: background temperature, θ_α: thermal bias). We apply the thermal gradient θ only to the left non-superconducting lead ($T_{\rm L} = T + \theta$) while the superconductor maintains the equilibrium temperature $T_{\rm S} = T$ ($\theta_{\rm S} = 0$) and take the Fermi level to be $E_{\rm F} = 0$. Thus, the forward thermal bias is defined by $\theta > 0$ and the backward one by $-T < \theta < 0$.

Importantly, the quasiparticle transmission in equation (7) is proportional to the superconducting density of states $\Theta(|\varepsilon| - \Delta)/\sqrt{\varepsilon^2 - \Delta^2}$, i.e.

$$T^\sigma_{\rm Q}(\varepsilon) \propto \Gamma_{{\rm L}\sigma}\Gamma_{\rm S}\frac{\Theta(|\varepsilon| - \Delta)|\varepsilon|}{\sqrt{\varepsilon^2 - \Delta^2}}, \tag{8}$$

where $\Gamma_{{\rm L}\sigma} = \Gamma_{\rm L}(1 + \sigma p) = 2\pi|t_{{\rm L}\sigma}|^2\sum_k \delta(\varepsilon - \varepsilon_{{\rm L}k\sigma})$ and $\Gamma_{\rm S} = 2\pi|t_{{\rm S}\sigma}|^2\sum_k \delta(\varepsilon - \varepsilon_{{\rm S}k\sigma})$ are the tunnel broadenings to each lead in the wide-band approximation, and $\Theta(\varepsilon)$ is the Heaviside step function, respectively. An explicit expression of $T^\sigma_{\rm Q}(\varepsilon)$ can be found in appendix. It clearly follows from equation (8) that due to the energy gap Δ of the superconducting lead, one needs to apply high enough (forward) thermal bias to the system in order to activate the quasiparticle contribution. On the other hand, the quasiparticle current can be deactivated when we cool the system down, i.e., applying backward thermal gradient with $\theta < 0$, in which case the current is highly suppressed. This comprises the working principle of our charge and spin Seebeck diode proposed here: (i) complete suppression of the parasitic Andreev current with $V = 0$, (ii) activation of quasiparticles above the superconducting gap with the forward temperature gradient $\theta > 0$ but not the other way round with $\theta < 0$.

Now, the combination of superconductivity and spintronics can lead to novel functionalities with better performances [33, 34]. In order to realize the spin Seebeck diode [2–6]. Either finite magnetic field $\Delta_Z \neq 0$ or a nonzero polarization $p \neq 0$ using the ferromagnet is necessary to break the spin symmetry of the transmission, viz. $T^{\uparrow}_{\rm Q}(\varepsilon) \neq T^{\downarrow}_{\rm Q}(\varepsilon)$ in equation (8). However, even in nonmagnetic case with $p = \Delta_Z = 0$, the charge current–temperature curves would clearly show the charge Seebeck diode features owing to the underlying mechanism explained above. Below, we discuss $I_{\rm c} - \theta$ and $I_{\rm s} - \theta$ characteristics in the isoelectric case where the charge ($I_{\rm c}$) and spin ($I_{\rm s}$) currents are defined with the aid of equation (7):

$$I_{\rm c} = I_{\uparrow} + I_{\downarrow}, \tag{9}$$

$$I_{\rm s} = I_{\uparrow} - I_{\downarrow}. \tag{10}$$

3. Results and discussion

We firstly discuss the interaction effects characterized by the screening potential. Figure 2 shows U_σ as a function of θ in a N–D–S device where $p = \Delta_Z = 0$. The potential U_σ for $\theta < 0$ is rather suppressed whereas it linearly increases for $\theta > 0$. In addition, its linear slope saturates as we increase the dot level beyond $\varepsilon_{\rm d} = 0.5\Delta$ close to the superconductor gap for $\theta > 0$ while the potential decreases further for $\theta < 0$ as $\varepsilon_{\rm d}$ approaches Δ. We emphasize that interaction effects are beneficial for the diode behavior discussed here since the forward thermal bias $\theta > 0$ shifts the effective dot level higher than that of noninteracting limit to keep the dot charge constant. This is a nice property that clearly makes the synergy with the thermally excited quasiparticle states in the left normal contact.

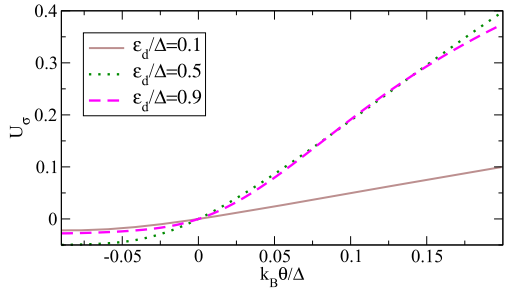

Figure 2. U_σ versus θ for several ε_d at $k_B T = 0.1\Delta$ and $p = \Delta_Z = 0$ with $\Gamma_N \ll \Gamma_S$.

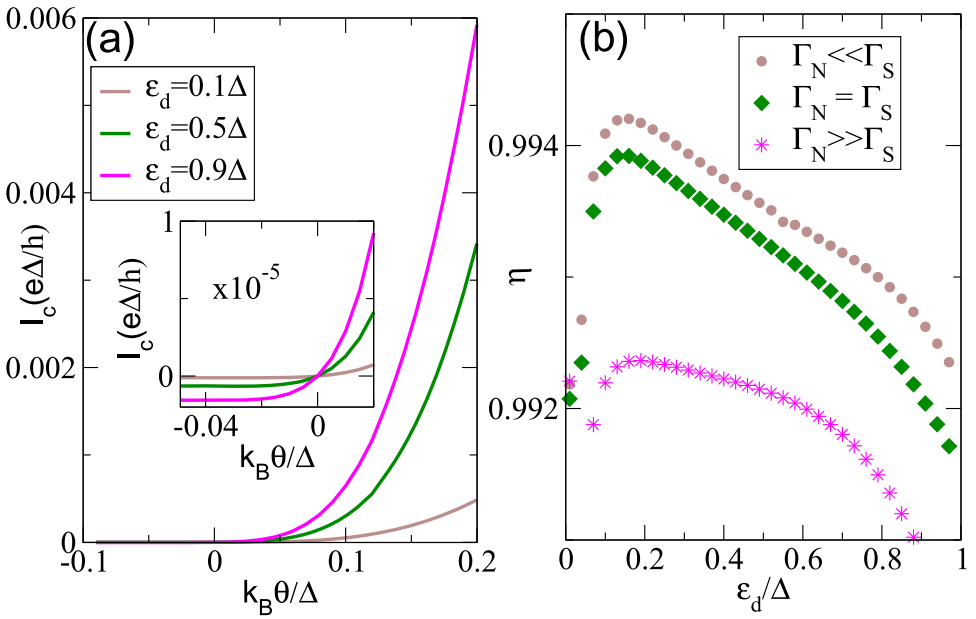

Figure 3. (a) I_c versus θ for several ε_d at $p = \Delta_Z = 0$. The case for $\Gamma_N \ll \Gamma_S$ is shown. (b) η versus ε_d at $k_B\theta_0 = 0.07\Delta$ for different coupling limits, where $\Gamma_N = 0.1\Delta$, $\Gamma_N = 0.3\Delta$, and $\Gamma_N = 0.5\Delta$ for each case while the total broadening is fixed, i.e., $\Gamma_N + \Gamma_S = 0.6\Delta$. The background temperature is $k_B T = 0.1\Delta$. Inset of (a) shows that the Ohmic region with $I_c(\theta) = -I_c(-\theta)$ is very narrow.

Figure 3 displays the charge Seebeck diode behavior of our hybrid device and its high rectification efficiency. For the moment, a purely nonmagnetic case $p = \Delta_Z = 0$ in a N–D–S setup is considered. In figure 3(a), the charge current for backward thermal gradients $\theta < 0$ is greatly suppressed as discussed above whereas strongly nonlinear thermocurrent is generated by heating ($\theta > 0$) the normal metallic lead. Moreover, the forward current can be amplified by tuning the gate potential as shown with several dot level positions. I_c increases as the dot level position approaches the superconducting gap onset and it is reinforced by interaction effects.

The rectification efficiency can be quantified by

$$\eta = \frac{|I_c(\theta_0)| - |I_c(-\theta_0)|}{|I_c(\theta_0)|} \tag{11}$$

for fixed forward and backward thermal gradients $\pm\theta_0$. This number is bounded and the maximum efficiency is given by $\eta = 1$ if the backward thermocurrent completely vanishes. In figure 3(b), η is shown as a function of ε_d at $k_B\theta_0 = 0.07\Delta$. This thermal bias is about 250 mK for Al, still lower than the background temperature. Therefore, we do not need large temperature bias to observe the diode effect (inset of figure 3(a)). Remarkably, the rectification is very efficient as η is close to unity for various coupling limits, i.e., stronger coupling to S or N and an identical tunnel broadening to each lead. This shows the robustness of our device to unintentional variations of the coupling values to the external contacts. Albeit not shown, high efficiencies displayed here are rather insensitive to the change of background temperature T. Another useful way of quantifying the efficiency of our device is to introduce the asymmetry ratio defined by

Table 1. Asymmetry ratio R for several ε_d and θ_0.

	$k_B\theta_0 = 0.01\Delta$	$k_B\theta_0 = 0.04\Delta$	$k_B\theta_0 = 0.07\Delta$
$\varepsilon_d = 0.1\Delta$	2.68	31	166
$\varepsilon_d = 0.5\Delta$	2.64	30	155
$\varepsilon_d = 0.9\Delta$	2.53	27	134

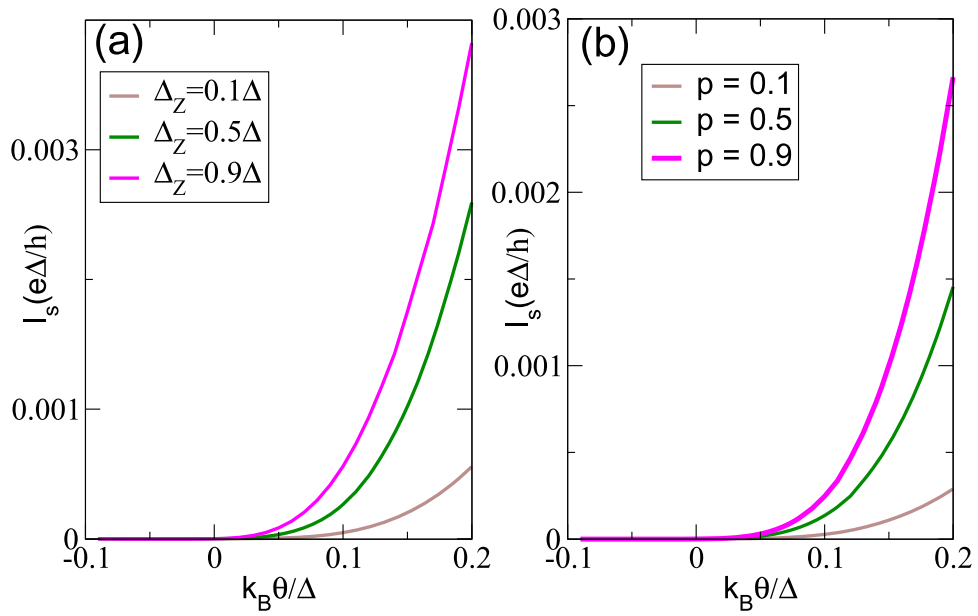

Figure 4. I_s versus θ at (a) $p = 0$ for several Δ_Z, and (b) $\Delta_Z = 0$ for several p. As shown in (a), spin Seebeck diode can be embodied even without a ferromagnetic lead. We have fixed $\varepsilon_d = 0.5\Delta$ and $k_B T = 0.1\Delta$ with $\Gamma_{N,F} \ll \Gamma_S$.

$$R = \frac{|I_c(\theta_0)|}{|I_c(-\theta_0)|}. \tag{12}$$

One can easily find the relation $R = 1/(1-\eta)$ from equation (11). Table 1 displays a fast growth of R as a function of θ_0, which can be inferred from figure 3.

Figure 4(a) shows the spin Seebeck diode feature [2–6] in a N–D–S device with a magnetic field applied to the dot, i.e., $\Delta_Z \neq 0$. The ferromagnet is not an essential ingredient if the Zeeman splitting in the dot is nonzero. We observe a quick increase of the spin current as a function of θ. This increase is more dramatic for higher Zeeman splitting because then the dot level allows for greater current into the empty quasiparticle states. In figure 4(b), a F–D–S setup with a nonzero polarization $p \neq 0$ also exhibits the spin current rectification depending on the thermal bias direction. In this case, I_s increases for higher p due to more available states with spin up in the source contact. The analogous rectification efficiencies (equation (11) but with $I_s(\pm\theta_0)$) for both figures 4(a) and (b) are also as high as the charge current counterpart (not shown here). Our results suggest that this Seebeck diode device based on the hybrid superconducting quantum dot is very efficient and versatile.

In a realistic superconductor sample, the energy gap depends on the temperature, e.g., $\Delta(T) = \Delta_0\sqrt{1-(T/T_c)^2}$, where T_c is the superconducting critical temperature of the material. If we take Al for a superconductor, its zero temperature energy gap is about $\Delta_0 = 0.34$ meV with $T_c = 1.2$ K. Then, one can easily estimate $\Delta(500\text{ mK}) \approx 0.9\Delta_0$ with the background temperature $k_B T = 0.1\Delta_0$ we have used in this paper. This means that Al superconducting gap is mostly unaffected up to rather high temperatures $T \approx 500$ mK. One can therefore practically embody the Seebeck diode as suggested here with, e.g., an Al superconductor and a nanowire or a carbon nanotube quantum dot. A typical current value is $0.001e\Delta/h \approx 13$ pA, which is within the reach of today's experimental techniques [17]. For the magnetic configurations, however, $\Delta_Z = 0.1\Delta$ corresponds to $B \approx 0.03$ T for a nanowire quantum dot with an effective g-factor 40. This already exceeds the critical field $B_c = 0.01$ T of Al, hence in this case a superconductor with a higher B_c, e.g., Nb compounds, should be used to observe the effects shown in figure 4(a).

4. Summary

Since thermoelectric generators and coolers have thus far shown low efficiencies, it is crucial to propose efficient thermoelectric devices with new purposes. Here, we have proposed a proof-of-principle design for a charge and spin Seebeck diode built from the hybrid superconductor quantum dot device. Either normal metallic or ferromagnetic lead can be attached to the quantum dot. Our device shows strong rectification and diode effects as the rectification efficiency is very close to 100%. We have found that the diode features in the device are highly tunable with back gate potentials, magnetic fields, and lead magnetizations which opens the route for its use in information processing applications.

We have treated Coulomb interactions in the mean-field approximation. In this case, the potential shift is a function of the temperature gradient applied to the non-superconducting lead. Our calculations are valid for metallic dots with good screening properties [23]. We expect that the diode behaviors would survive for a broad range of interaction strengths, even beyond mean field, since the main underlying mechanism of rectification effects is the gapped quasiparticle spectrum with a complete suppression of the subgap transport.

Acknowledgments

The authors acknowledge the support from MINECO under Grant No. FIS2014-52564 and the Korean NRF under Grant No. 2014R1A6A3A03059105.

Appendix. Green's functions and quasiparticle transmission

In the isoelectric case with $V = 0$, the lesser Green's functions are given by

$$\begin{aligned} G^<_\uparrow(\varepsilon) &= \frac{\mathrm{i}}{2\pi} f_{\mathrm{L}}(\varepsilon)[\Gamma_{\mathrm{L}\uparrow}|G^r_{11}(\varepsilon)|^2 + \Gamma_{\mathrm{L}\downarrow}|G^r_{12}(\varepsilon)|^2] \\ &\quad + \frac{\mathrm{i}\widetilde{\Gamma}_{\mathrm{S}}}{2\pi} f_{\mathrm{S}}(\varepsilon)\left[|G^r_{11}(\varepsilon)|^2 + |G^r_{12}(\varepsilon)|^2 - \frac{2\Delta}{|\varepsilon|}\mathrm{Re}\,[G^r_{11}(\varepsilon)G^{r,*}_{12}(\varepsilon)]\right], \end{aligned} \tag{A.1}$$

$$\begin{aligned} G^<_\downarrow(\varepsilon) &= \frac{\mathrm{i}}{2\pi} f_{\mathrm{L}}(\varepsilon)[\Gamma_{\mathrm{L}\downarrow}|G^r_{33}(\varepsilon)|^2 + \Gamma_{\mathrm{L}\uparrow}|G^r_{34}(\varepsilon)|^2] \\ &\quad + \frac{\mathrm{i}\widetilde{\Gamma}_{\mathrm{S}}}{2\pi} f_{\mathrm{S}}(\varepsilon)\left[|G^r_{33}(\varepsilon)|^2 + |G^r_{34}(\varepsilon)|^2 + \frac{2\Delta}{|\varepsilon|}\mathrm{Re}\,[G^r_{33}(\varepsilon)G^{r,*}_{34}(\varepsilon)]\right], \end{aligned} \tag{A.2}$$

where $\Gamma_{\mathrm{L}\sigma} = \Gamma_{\mathrm{L}}(1 + \sigma p)$ and $\widetilde{\Gamma}_{\mathrm{S}} = \Gamma_{\mathrm{S}}\Theta(|\varepsilon| - \Delta)|\varepsilon|/\sqrt{\varepsilon^2 - \Delta^2}$. Then, the spin-generalized charge fluctuations in equation (5) can be written as

$$\delta q_\uparrow = -\mathrm{i}\int \mathrm{d}\varepsilon\,[G^<_\uparrow(\varepsilon) - G^<_{\uparrow,\mathrm{eq}}(\varepsilon)], \tag{A.3}$$

$$\delta q_\downarrow = -\mathrm{i}\int \mathrm{d}\varepsilon\,[G^<_\downarrow(\varepsilon) - G^<_{\downarrow,\mathrm{eq}}(\varepsilon)], \tag{A.4}$$

for each spin, respectively, where $G^<_{\sigma,\mathrm{eq}}(\varepsilon)$ is the value of $G^<_\sigma(\varepsilon)$ at thermal equilibrium. The retarded Green's functions which we have used in the above expressions are explicitly given by

$$G^r_{11}(\varepsilon) = \left[\varepsilon - \tilde{\varepsilon}_{\mathrm{d}\uparrow} + \frac{\mathrm{i}\Gamma_{\mathrm{L}\uparrow}}{2} + \frac{\mathrm{i}\Gamma_{\mathrm{S}}}{2}\beta_{\mathrm{d}}(\varepsilon) + \frac{\Gamma_{\mathrm{S}}^2\Delta^2}{4(\varepsilon^2 - \Delta^2)}A^r_1(\varepsilon)\right]^{-1}, \tag{A.5}$$

$$G^r_{33}(\varepsilon) = \left[\varepsilon - \tilde{\varepsilon}_{\mathrm{d}\downarrow} + \frac{\mathrm{i}\Gamma_{\mathrm{L}\downarrow}}{2} + \frac{\mathrm{i}\Gamma_{\mathrm{S}}}{2}\beta_{\mathrm{d}}(\varepsilon) + \frac{\Gamma_{\mathrm{S}}^2\Delta^2}{4(\varepsilon^2 - \Delta^2)}A^r_2(\varepsilon)\right]^{-1}, \tag{A.6}$$

$$G^r_{12}(\varepsilon) = G^r_{11}(\varepsilon)\frac{\mathrm{i}\Gamma_{\mathrm{S}}}{2}\beta_o(\varepsilon)A^r_1(\varepsilon), \tag{A.7}$$

$$G^r_{34}(\varepsilon) = -G^r_{33}(\varepsilon)\frac{\mathrm{i}\Gamma_{\mathrm{S}}}{2}\beta_o(\varepsilon)A^r_2(\varepsilon), \tag{A.8}$$

with

$$A^r_1(\varepsilon) = \left[\varepsilon + \tilde{\varepsilon}_{\mathrm{d}\downarrow} + \frac{\mathrm{i}\Gamma_{\mathrm{L}\downarrow}}{2} + \frac{\mathrm{i}\Gamma_{\mathrm{S}}}{2}\beta_{\mathrm{d}}(\varepsilon)\right]^{-1}, \tag{A.9}$$

$$A^r_2(\varepsilon) = \left[\varepsilon + \tilde{\varepsilon}_{\mathrm{d}\uparrow} + \frac{\mathrm{i}\Gamma_{\mathrm{L}\uparrow}}{2} + \frac{\mathrm{i}\Gamma_{\mathrm{S}}}{2}\beta_{\mathrm{d}}(\varepsilon)\right]^{-1}, \tag{A.10}$$

$$\beta_{\rm d}(\varepsilon) = \frac{\Theta(|\varepsilon| - \Delta)|\varepsilon|}{\sqrt{\varepsilon^2 - \Delta^2}} - {\rm i}\frac{\Theta(\Delta - |\varepsilon|)\varepsilon}{\sqrt{\Delta^2 - \varepsilon^2}}, \tag{A.11}$$

$$\beta_{o}(\varepsilon) = \frac{\Theta(|\varepsilon| - \Delta){\rm sgn}(\varepsilon)\Delta}{\sqrt{\varepsilon^2 - \Delta^2}} - {\rm i}\frac{\Theta(\Delta - |\varepsilon|)\Delta}{\sqrt{\Delta^2 - \varepsilon^2}}, \tag{A.12}$$

where $\tilde{\varepsilon}_{{\rm d}\sigma} = \varepsilon_{{\rm d}\sigma} + U_\sigma$ represents the renormalized quantum dot level by spin-dependent interaction U_σ (see equation (4)).

With explicit expressions for the retarded Green's functions, the spin-dependent quasiparticle transmission in equation (8) is given by

$$T_Q^{\uparrow}(\varepsilon) = \Gamma_{{\rm L}\uparrow}\tilde{\Gamma}_{\rm S}\left(|G_{11}^r(\varepsilon)|^2 + |G_{12}^r(\varepsilon)|^2 - \frac{2\Delta}{|\varepsilon|}{\rm Re}\left[G_{11}^r(\varepsilon)G_{12}^{r,*}(\varepsilon)\right]\right), \tag{A.13}$$

$$T_Q^{\downarrow}(\varepsilon) = \Gamma_{{\rm L}\downarrow}\tilde{\Gamma}_{\rm S}\left(|G_{33}^r(\varepsilon)|^2 + |G_{34}^r(\varepsilon)|^2 + \frac{2\Delta}{|\varepsilon|}{\rm Re}\left[G_{33}^r(\varepsilon)G_{34}^{r,*}(\varepsilon)\right]\right), \tag{A.14}$$

for each spin where $\tilde{\Gamma}_{\rm S} = \Gamma_{\rm S}\Theta(|\varepsilon| - \Delta)|\varepsilon|/\sqrt{\varepsilon^2 - \Delta^2}$.

References

[1] Li B, Wang L and Casati G 2004 *Phys. Rev. Lett.* **93** 184301
[2] Ren J and Zhu J-X 2013 *Phys. Rev.* B **88** 094427
[3] Borlenghi S, Wang W, Fangohr H, Bergqvist L and Delin A 2014 *Phys. Rev. Lett.* **112** 047203
[4] Borlenghi S, Lepri S, Bergqvist L and Delin A 2014 *Phys. Rev.* B **89** 054428
[5] Ren J, Fransson J and Zhu J-X 2014 *Phys. Rev.* B **89** 214407
[6] Fu H-H, Wu D-D, Gu L, Wu M and Wu R 2015 *Phys. Rev.* B **92** 045418
[7] Uchida K, Takahashi S, Harii K, Ieda J, Koshibae W, Ando K, Maekawa S and Saitoh E 2008 *Nature* **455** 778
[8] Slachter A, Bakker F L, Adam J-P and van Wees B J 2010 *Nat. Phys.* **6** 879
[9] Bauer G E W, MacDonald A H and Maekawa S 2010 *Solid State Commun.* **150** 459
[10] Fahlvik Svensson S, Hoffmann E A, Nakpathomkun N, Wu P M, Xu H Q, Nilsson H A, Sánchez D, Kashcheyevs V and Linke H 2013 *New J. Phys.* **15** 105011
[11] Sierra M A and Sánchez D 2014 *Phys. Rev.* B **90** 115313
[12] Sánchez D and López R 2013 *Phys. Rev. Lett.* **110** 026804
[13] Hwang S-Y, López R, Lee M and Sánchez D 2014 *Phys. Rev.* B **90** 115301
[14] Jiang J-H, Kulkarni M, Segal D and Imry Y 2015 *Phys. Rev.* B **92** 045309
[15] Hwang S-Y, López R and Sánchez D 2016 *Phys. Rev.* B **94** 054506
[16] Ozaeta A, Virtanen P, Bergeret F S and Heikkila T T 2014 *Phys. Rev. Lett.* **112** 057001
[17] Kolenda S, Wolf M J and Beckmann D 2016 *Phys. Rev. Lett.* **116** 097001
[18] Kalenkov M S and Zaikin A D 2014 *Phys. Rev.* B **90** 134502
[19] Machon P, Eschrig M and Belzig W 2014 *New J. Phys.* **16** 073002
[20] Büttiker M 1993 *J. Phys.: Condens. Matter* **5** 9361
[21] Whitney R S 2013 *Phys. Rev.* B **87** 115404
[22] Meair J and Jacquod P 2013 *J. Phys.: Condens. Matter* **25** 082201
[23] Brouwer P W, Lamacraft A and Flensberg K 2005 *Phys. Rev.* B **72** 075316
[24] Lo S-T, Chen K Y, Lin S-D, Wu J-Y, Lin T L, Yeh M R, Chen T-M and Liang C-T 2013 *Sci. Rep.* **3** 2274
[25] Gräber M R, Nussbaumer T, Belzig W and Schönenberger C 2004 *Nanotechnology* **15** S479
[26] Deacon R S, Tanaka Y, Oiwa A, Sakano R, Yoshida K, Shibata K, Hirakawa K and Tarucha S 2010 *Phys. Rev. Lett.* **104** 076805
[27] Cao X, Shi Y, Song X, Zhou S and Chen H 2004 *Phys. Rev.* B **70** 235341
[28] Wang J, Wei Y, Guo H, Sun Q- F and Lin T- H 2001 *Phys. Rev.* B **64** 104508
[29] López R, Lim J S and Sánchez D 2012 *Phys. Rev. Lett.* **108** 246603
[30] Cuevas J C, Martín-Rodero A and Levy Yeyati A 1996 *Phys. Rev.* B **54** 7366
[31] Sun Q-F, Wang J and Lin T-H 1999 *Phys. Rev.* B **59** 3831
[32] Hwang S-Y, López R and Sánchez D 2015 *Phys. Rev.* B **91** 104518
[33] Linder J and Robinson J W A 2015 *Nat. Phys.* **11** 307
[34] Linder J and Bathen M E 2016 *Phys. Rev.* B **93** 224509